

HIGH TEMPERATURE CREEP OF Ru-BEARING Ni-BASE SINGLE CRYSTAL SUPERALLOYS

AC Yeh, CMF Rae and S Tin
Department of Materials Science and Metallurgy, University of Cambridge, Cambridge CB2 3QZ, UK

Keywords: Rafting, TCP phases, Lattice misfit, interfacial dislocations, Ruthenium

Abstract

The response of high-refractory content Ni-base superalloys to high temperature creep deformation is primarily governed by microstructural changes. The present study investigates the creep behavior of advanced Ru containing single crystal superalloys. The main observation is that the improved stability provided by Ru additions hinders the formation of Topologically-Close-Packed (TCP) precipitates. Comparison of two nominally similar alloys with and without Ru reveals that the phase stability exhibited by the Ru containing alloy significantly improves the high temperature creep resistance. Ruptured and interrupted creep tests were carried out and studies related to high temperature creep mechanisms were performed. Microstructural investigations using scanning electron microscope (SEM) and transmission electron microscope (TEM) yielded information pertaining to the kinetics of rafting, TCP precipitate formation, γ'/γ lattice misfit, and compositional changes occurring at various stage of creep deformation. The primary mechanism associated with the improvement in high temperature creep resistance is attributed to the enhanced phase stability in Ru-bearing single crystal superalloys.

Introduction

Nickel-base single crystal superalloys are predominately used as materials for turbine blades in aero-engines because they exhibit excellent mechanical properties at elevated temperatures. Continual improvements in the mechanical response of superalloys have coincided with an improved understanding of the high temperature deformation mechanisms and the addition of refractory elements, such as Re, W and Mo to enhance the degree of solid-solution strengthening. Morphological changes of the γ'/γ microstructure in conventional single crystal Ni-base superalloys during long-term deformation at high temperature result in directional coarsening of the γ' and the formation of "rafts" aligned perpendicular to the applied stress direction [1]. Under certain loading conditions, the rafted microstructure can be an effective barrier to continued deformation. Studies have suggested that the onset of steady state creep at high temperatures and low stresses corresponds to the completion of rafting in the microstructure [2]. The driving force for rafting depends on the high temperature diffusion, lattice misfit, properties of γ'/γ and the applied stress [3]. Although the addition of refractory elements can strengthen both γ and γ' phases, they tend to promote the formation of intermetallic TCP phases, such as σ , P, μ or R [4, 5, 6], that eventually degrade the mechanical properties after long-term exposure at elevated temperatures [7, 8]. Recent studies have shown that additions of the platinum group metal; ruthenium may potentially increase the microstructural stability and creep resistance of these unique alloys [9, 10].

In the present investigation, two experimental single crystal Ni-base superalloys – RR2100 and RR2101 were selected to study the effect of Ru on high temperature creep behaviour. Previous findings have shown that the Ru addition alters the solidification characteristics and greatly enhances the phase stability of RR2101 [11]. Since high temperature creep properties are dependent upon the stability of the microstructure at elevated temperatures, Ru additions are expected to indirectly influence high temperature creep properties.

High temperature creep behavior of single crystal nickel base superalloys are influenced by factors such as the kinetics of rafting, stability of the rafted γ'/γ microstructure, formation of TCP precipitates, and changes in γ'/γ volume fraction. Detailed studies on each of these aspects were carried out to establish the role of Ru during high temperature creep of advanced Ni-base superalloys.

Experiments

Single crystal specimens of RR2100 and RR2101 alloys were cast by Rolls-Royce as 12.7mm diameter cylindrical bars with orientations within 15 degrees of the $\langle 001 \rangle$ orientation. The bars were solution-treated using the standard CMSX-10 solution treatment. It comprised of a long, ramped cycle rising in steps to 1364°C, at which temperature the material was held for 20 hours, and then followed by a primary age of 5 hours at 1140°C and secondary age of 16 hours at 870°C. The compositions of these alloys are listed in Table I. Due to the elevated level of refractory alloying additions, RR2100 was revealed to be an inherently unstable alloy with respect to the formation of TCP phases. RR2101 is nominally identical to RR2100 with the exception of the 2wt% Ru, which was substituted for nickel. The following experiments were carried out to characterize the high temperature creep response for both alloys.

Table I. Chemical Compositions of RR2100 and RR2101 (wt %)

Alloy	Co	Cr	W	Re	Ru	Al	Ta	Ni
RR2100	12	2.5	9	6.4	0	6	5.5	Bal.
RR2101	12	2.5	9	6.4	2	6	5.5	Bal.

Creep Tests

Solution-treated and aged RR2100 and RR2101 were machined into standard creep specimens and tested along the [001] direction to rupture under the following five conditions: (1) 1100°C/100MPa, (2) 1100°C/150MPa, (3) 1100°C/175MPa, (4) 1000°C/275MPa and (5) 1000°C/400MPa. In addition, a series of

interrupted creep tests were performed for both alloys at 1100°C to monitor the microstructural changes during deformation.

Optical and SEM Metallography

Crept specimens of RR2100 and RR2101 were observed under both the optical microscope and JEOL 5800LV scanning electron microscope (SEM) to assess the degree of microstructural rafting and volume fraction of TCP phase precipitation. Samples were sectioned in both horizontal and vertical directions with respect to the tensile axis and prepared using standard metallographic techniques, with a final polish of colloidal silica. The general purpose etching solution for the single crystal superalloy - Nimonic (80ml HCL, 20ml H₂O, 2ml HNO₃ and 16grams FeCl₃) was used to reveal the microstructures. Volume fraction analyses of phases contained within the microstructures were performed using KS300 software.

TEM Dislocation and γ'/γ Compositional Analysis

Crept specimens were cut into thin disks (~0.4mm in thickness) perpendicular to the [001] direction. The disks were then mechanically ground to ~0.1mm in thickness, and electrochemically thinned using a twin-jet polisher with a solution of 10% perchloric acid in methanol between -2°C to -3°C for RR2100 and -5°C to -7°C for RR2101. A JEOL 2000FX transmission electron microscope (TEM) was used to carry out dislocation analysis. Studies were based on a minimum of three TEM samples for every creep condition to ensure a representative dislocation structure was observed.

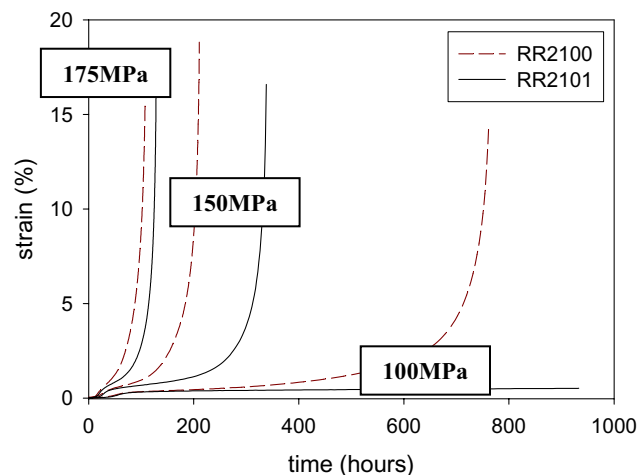


Figure 1. Comparison of creep behavior at 1100°C. Under 100MPa, RR2100 ruptured while RR2101 still remained at steady state creep; the creep test for RR2101 was then interrupted. As the load increases to 150MPa and 175MPa, the effect of Ru addition is less pronounced.

A FEI Tecnai F20-G2 FEGTEM was used to carry out compositional analysis on γ and γ' in as-solutioned and crept specimens. The FEI Tecnai F20 has 200kV field emission gun (FEG), high resolution and analytical TEM/STEM capability.

Lattice Misfit Measurements

A Rigaku Geigerflex ($\theta/2\theta$) vertical X-ray diffractometer was used to obtain characteristic γ'/γ peaks from as-solutioned RR2100 and RR2101. The hot stage of the diffractometer allows the scans to be performed at high temperatures (<1400°C) within a vacuum environment $\sim 1 \times 10^{-6}$ atm. Specimens were carefully machined into the specified dimensions and inserted into a Pt holder to minimize displacement error. The x-ray scans were collected with the anode generator set at 40kV and 150mA.

Scans were performed at room temperature, 900°C and 1100°C for both RR2100 and RR2101. Philips PROFIT software was used for accurate determination of peak positions for the constituent γ' and γ phases. The results were also used to estimate the lattice misfit for each alloy at different temperatures.

TCP Characterization

Isothermal exposures at 1180°C were carried out on as-solutioned samples to induce TCP precipitation in both RR2100 and RR2101. Due to the orientation relationship between TCP phases and the matrix, samples were sectioned along the {111} plane of the γ'/γ matrix so that diffraction patterns can be used to reveal the characteristic crystal structures of the various TCP phases. The FEI Tecnai F20 was also used to determine the chemical composition of those TCP phases.

Results and Analysis

Single crystal specimens of RR2100 and RR2101 were subjected to constant load creep deformation over a range of stresses at 1000°C and 1100°C. Although similar at the other conditions, Figure 1 shows that the creep response of RR2100 and RR2101 differ significantly at 1100°C and 100MPa. Under these conditions, the total creep strain accumulated in RR2100 was approximately 15%, while the creep test for RR2101 was interrupted with an accumulated strain of less than 1% after approximately 900 hours. However, as the load was increased to 150MPa, the differences in creep performance are reduced as RR2101 only exhibits a slightly longer creep rupture life than RR2100. Figure 1 also shows that the overall creep strain for RR2100 and RR2101 at 1100°C and 150MPa was measured to be approximately 18% and 15% respectively. As the load increased to 175MPa, the creep response of RR2100 and RR2101 was revealed to be almost identical with accumulated strain around 15% for both alloys. Figure 2 shows the comparison of the creep properties of RR2100 and RR2101 at 1000°C 275MPa and 400MPa. Under these conditions, the creep behavior in terms of rupture lives and strains of the two experimental alloys are also very similar.

Minimum creep strain rates of RR2100 and RR2101 at 1100°C creep tests were obtained by plotting creep strain rate vs. accumulated strain, values are shown in Figure 3. Interestingly, RR2101 exhibits lower minimum creep strain rates than RR2100 under all of these creep conditions investigated. As the load increases from 100MPa to 175MPa, the minimum creep strain rate increases for both alloys. The difference in minimum creep strain rates between RR2100 and RR2101, however, is maintained.

Microstructural Evolution

Microstructures of the two experimental alloys after high temperature creep deformation are shown in Figures 4 and 5. After 120 hours at 1100°C 100MPa respectively, complete rafting of the microstructure had occurred and significant fractions of TCP phases were observed in RR2100, Figure 4(a). Although the Ru-bearing alloy, RR2101, was also observed to exhibit a rafted structure under the same condition, Figure 4(b), the microstructure was free of TCP phases. Spacing between the rafted structures in both alloys were measured to be $\sim 0.45\mu\text{m}$.

Figure 4(c) and 4(d) shows the microstructures of RR2100 (after rupture) and RR2101 (after approximately 900hours) under 1100°C 100MPa. Substantial coarsening of the rafted structure has occurred in RR2100, while the fine rafted structure in RR2101 remained unchanged with raft spacings still around $0.45\mu\text{m}$.

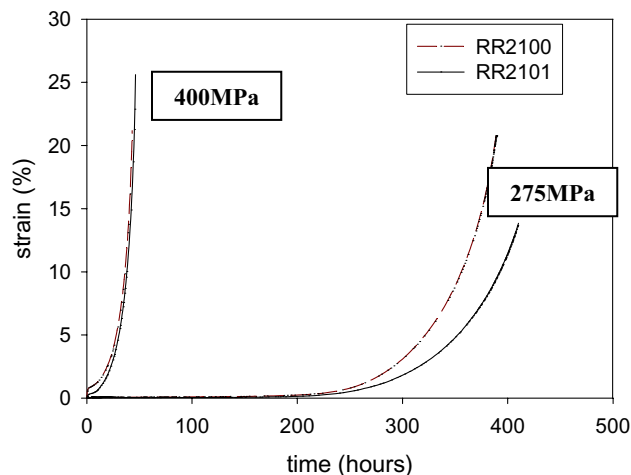


Figure 2. Comparison of creep behaviour at 1000°C, stress rupture responses are very similar between RR2100 and RR2101 under both 275MPa and 400MPa loads.

Figure 5(a) and (b) reveal that RR2100 and RR2101 have almost identical microstructures after creep at 1100°C 175MPa. Dislocation analyses were carried out on all crept samples. TEM bright field images of RR2100 and RR2101 after an interrupted creep test at 120hours under 1100°C 100MPa show that the interfacial dislocations are slightly finer in RR2101 than in RR2100. Statistically significant measurements were averaged over a minimum of five TEM specimens and are consistent over the range of temperatures and stresses investigated, Figure 3. This observation is consistent with studies reported by Zhang [12] on similar Ru-containing Ni-base superalloys. Dislocation networks in both alloys are aligned with the $\langle 100 \rangle$ orientations of the matrix with burgers vectors parallel to $[110]$. Figure 6 shows that dislocations present in the γ'/γ interface are primarily edge dislocations arranged in octahedral or square configurations.

Increased dislocation activity at the γ'/γ and TCP/ γ' interfaces was observed in RR2100. Compared to RR2100, few dislocations were observed in RR2101, Figure 6(b).

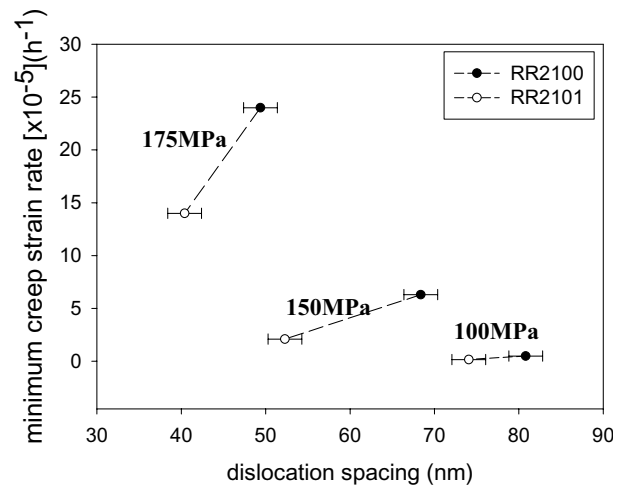


Figure 3. Minimum creep strain rates vs average dislocation spacings under 100MPa, 150MPa and 175MPa at 1100°C. RR2101 exhibits lower minimum creep strain rates than RR2100 in all conditions. As the stress increases, averaged dislocation spacing decreases and minimum creep strain rate increases. RR2101 is also found to have finer dislocations than RR2100 in all conditions.

TEM bright field images of RR2100 and RR2101 after creep rupture under 1100°C 150MPa are shown in Figure 7. The dominant dislocations identified in γ' again exhibit a screw character with $b=\langle 011 \rangle$, and the cutting of γ' is via pairs of dislocations separated by an anti-phase boundary (APB). In RR2100, cutting of γ' was observed mainly adjacent to TCP precipitates. Observations on samples crept under 175MPa show a very similar dislocation morphology.

Lattice Misfit Analysis

Philips PROFIT software was used to profile fit the $\{001\}$ peak position, which corresponds to the characteristic peak of γ' . The measured γ' positions were then used to deconvolute the $\{002\}$ superlattice reflection and determine peak position corresponding to γ . The subsequent lattice misfit was then estimated for each alloy at different temperatures.

The addition of Ru was found to influence the lattice parameter of γ more than γ' . Lattice parameters of γ were measured to be larger than γ' at room temperature for both alloys, Figure 8(a). Since the lattice misfit starts as negative at room temperature, Figure 8(b), misfit values of RR2100 and RR2101 become more negative as temperatures increase. For RR2100, misfit values range from -0.093% at room temperature to -0.242% at 1100°C. Misfit values for RR2101 range from -0.16% at room temperature to -0.281% at 1100°C. The results indicate RR2101 has an intrinsically higher misfit at all temperatures, especially at 900°C when compared to RR2100. Consistent with the XRD analysis, lattice images of γ'/γ were also taken to estimate the lattice misfit present in the two alloys to confirm the negative misfit at room temperature.

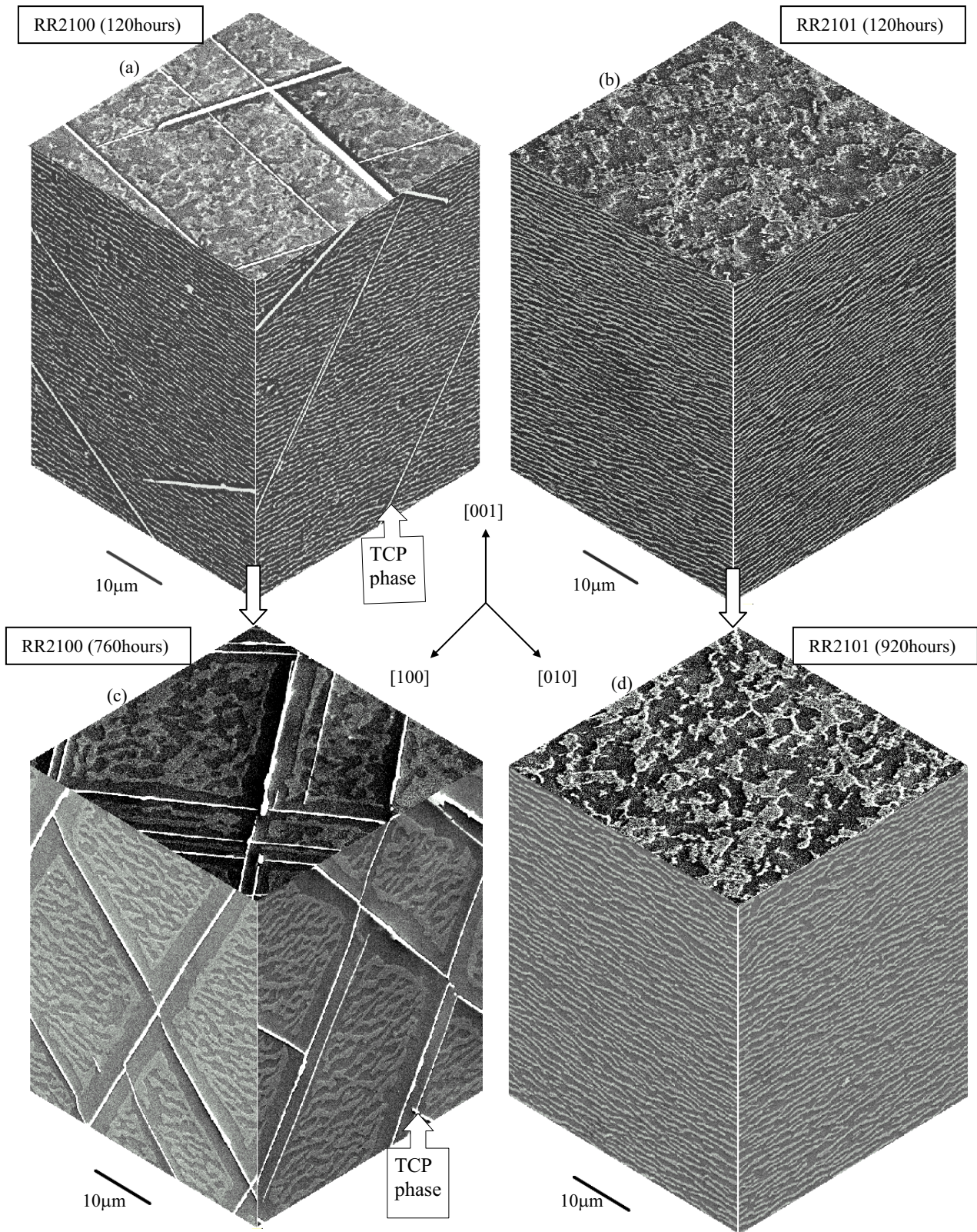


Figure 4. Images show microstructural evolution of RR2100 and RR2101 during creep at 1100°C 100MPa. (a) RR2100 and (b) RR2101 were interrupted at 120hours. (c) RR2100 was ruptured at 760hours with $\epsilon = 14\%$, (d) RR2101 was interrupted at 920hours with $\epsilon = 0.5\%$, and average raft spacing remains stable around $0.45\mu\text{m}$. (SEM (BEI) images)

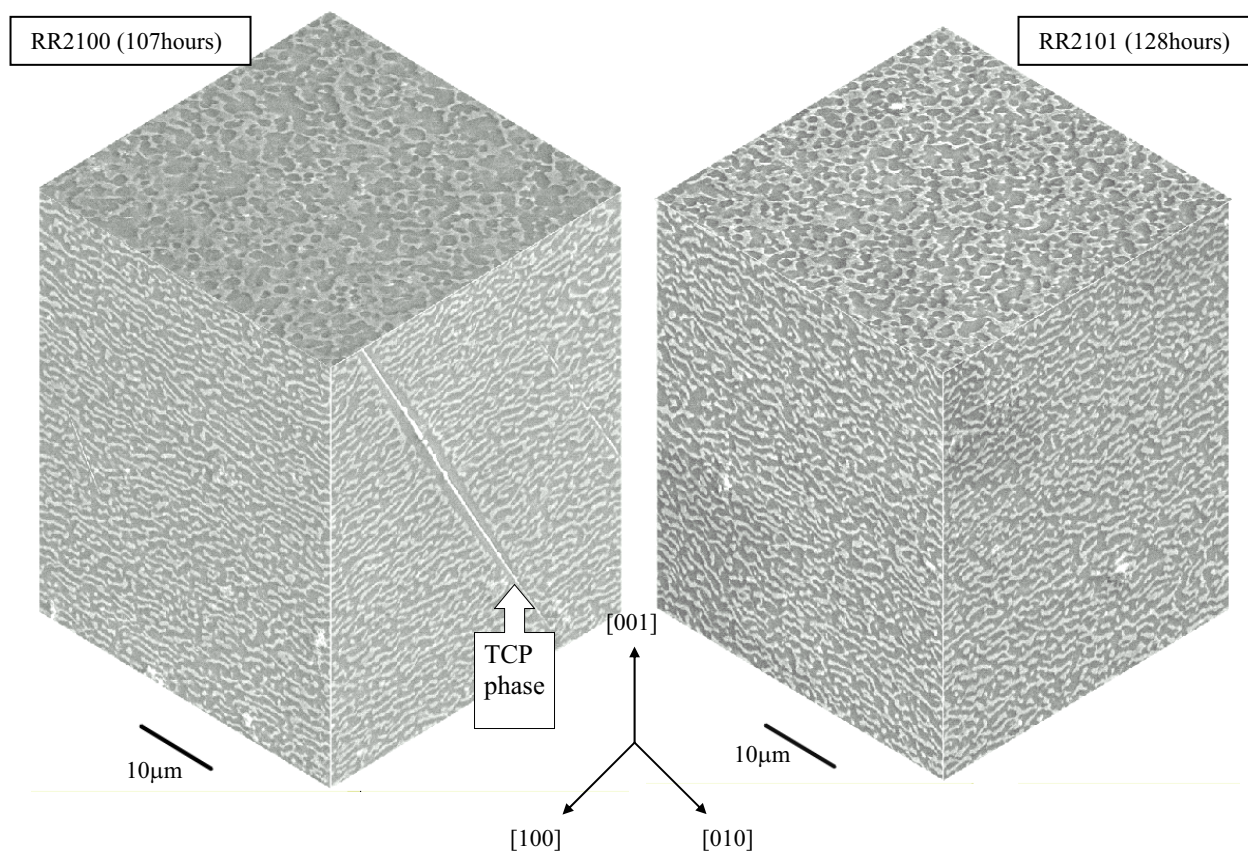


Figure 5. SEM (BEI) images of RR2100 and RR2101 after creep to rupture under 1100°C 175MPa. Both microstructures are almost identical.

γ'/γ Compositional Analysis

Compared to RR2100, the compositions of the constituent γ'/γ phases are not significantly altered with the addition of Ru, Figure 9. In RR2101, Ru partitions preferentially to the γ phase. These observations are consistent with results from lattice parameter measurements. All γ'/γ TEM-EDX scans were subjected to back calculation using the relative volume fraction of γ' and γ to ensure the validity of those results. TEM-EDX analysis of bulk γ' extractions were shown to be consistent with the wet chemical analysis and atom probe microanalysis [13] on RR2100 and RR2101.

Crept specimens were also subjected to TEM-EDX analysis of γ' phases adjacent to TCP precipitates. The results indicate that rafted γ' adjacent to TCP phases has the same composition as the γ' in the as-solutioned and aged specimens.

TCP Phase Characterization

Characterization of TCP phases present in these alloys was carried out after isothermal ageing RR2100 and RR2101 at 1180°C for 150 hours and 320 hours respectively. Substantially longer isothermal ageing time was required due to the sluggish precipitation kinetics in RR2101. Based on diffraction patterns taken from TCP phases aligned parallel to the $\{111\}$ of the γ'/γ matrix, the precipitates were identified as σ and P phases. P is the major TCP phase in both alloys. Interestingly, TEM-EDX results on P phase

in RR2100 and RR2101 show that Ru is absent from the TCP phases, Figure 10.

Discussion

At elevated temperatures, the creep resistance of single crystal Ni-base superalloys is dependent upon a number of factors including phase stability, lattice misfit and degree of solid solution strengthening in the γ and γ' phases. Results have shown that each of these factors is affected by the addition of Ru. The implications of these associated changes are discussed with respect to the results presented in this study.

During creep deformation at elevated temperatures, the microstructure of Ni-base single crystal superalloys can evolve from discrete cuboidal precipitates embedded in a γ matrix to coarse rafted structures. The rafted structure can be an effective barrier confining dislocation activity within the discrete γ rafts leading to steady state creep [2].

However, when the precipitation of TCP phase occurs within the system, solid solution strengthening elements, such as Re and W, are depleted from the γ matrix, leading to an extensive envelope of γ' around the TCP which may potentially act as a channel for preferential deformation. This is also associated with accelerated coarsening of the rafted structure in the proximity of the TCP precipitates. Thus, precipitation of TCP phases is detrimental to mechanical properties.

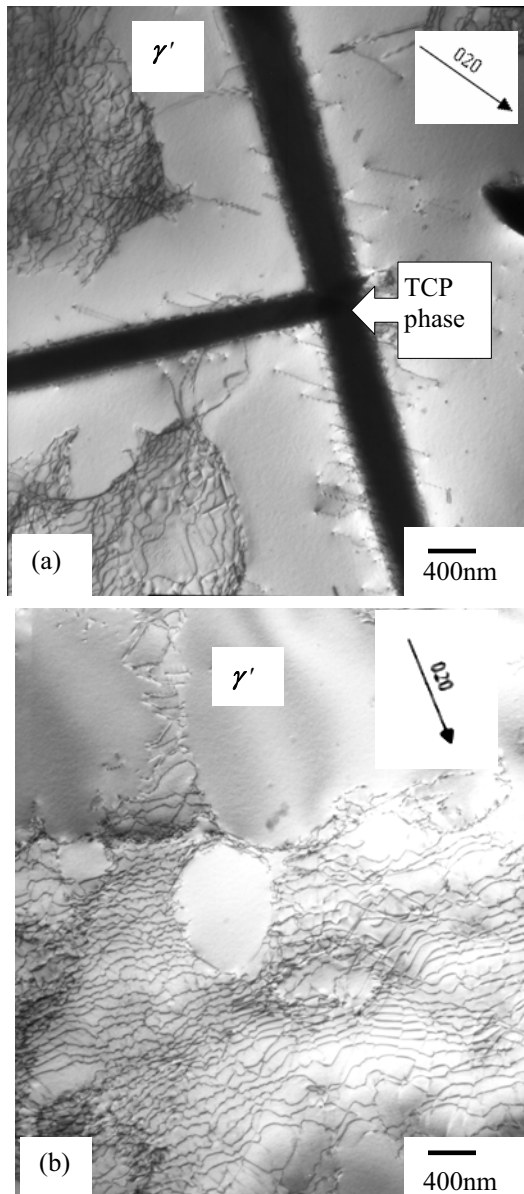


Figure 6. TEM bright field images of interrupted creep tests at 1100°C 100MPa. (a) RR2100, majority of dislocations in γ' observed are adjacent to TCP phases. As for γ' non-adjacent to TCP phases, little dislocations were observed. These dislocations in γ' are dominantly along the $\langle 011 \rangle$ or $\langle 101 \rangle$ direction. (b) RR2101, no TCP was observed and very few dislocations were observed in γ' .

At 1100°C 100MPa, the creep response of RR2100 and RR2101 was almost identical during the initial 120hours, Figure 1. Although some precipitation of TCP phases had occurred in RR2100 after 120hours, the volume fraction of TCP phases was low and both alloys exhibited similar raft spacings, Figure 4(a) and (b). During subsequent creep deformation, precipitation of TCP phases surrounded by a γ' matrix in RR2100 disrupted the stable rafted microstructure and enabled continuous creep deformation to occur, Figure 4(c).

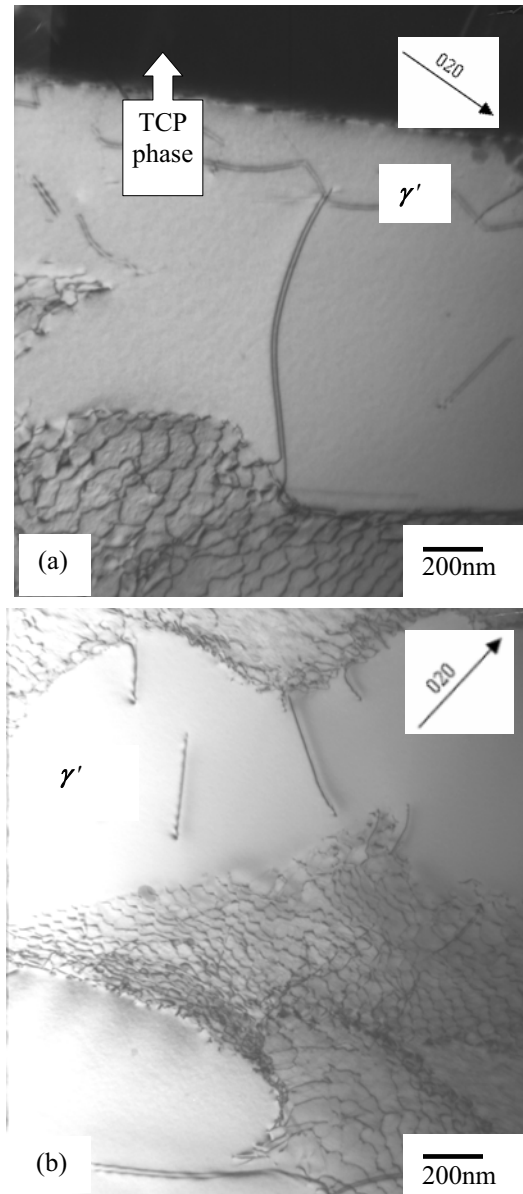


Figure 7. TEM bright field images of ruptured creep tests under 1100°C 150MPa. (a) RR2100, majority of dislocations in γ' observed are adjacent to TCP phases. As for γ' non-adjacent to TCP phases, some dislocations were observed. (b) RR2101, no TCP was observed and some dislocations were observed in γ' . $a/2\langle 011 \rangle$ and $a/2\langle 101 \rangle$ are the main dislocations observed in γ' for both alloys

Dislocation analysis revealed the presence of dislocations in γ' adjacent to TCP phases in RR2100, Figure 6 and 7. These interfacial dislocations are likely to be accommodating the crystallographic differences between the TCP and γ' phases and potentially serve as dislocation sources for deformation of γ' during tertiary creep. Both of these microstructural changes contribute to the rapid failure of RR2100.

Table II. Comparisons of overall γ' vol% within the matrix at various stages of creep and conditions. [At 1100°C 100MPa (750hours), the volume fraction of TCP phases become significant (~4.5 vol%) in RR2100.] (a) The overall γ' phase vol%. (b) The γ' vol% fractions in rafted regions that are not disrupted by TCP precipitation.]

	Pre-crept	1000°C 275MPa (>350hours)	1100°C 100MPa (120hours)	1100°C 100MPa (>750hours)		1100°C 150MPa (>200hours)	1100°C 175MPa (>100hours)
RR2100(γ')	74.60%	71.80%	66.10%	(a) 59.5%	(b) 42.12%	64.78%	65.09%
RR2101(γ')	74.30%	71.56%	66.09%	65.79%		67.84%	65.70%

On the other hand, RR2101 exhibited a greater resistance to the formation of TCP phases than RR2100 and was therefore able to maintain a stable rafted microstructure even after 900hours at 1100°C 100MPa. Thus, the Ru-containing alloy RR2101 was highly resistant to deformation at 100MPa, Figure 4(d). Preventing TCP precipitation and maintaining a stable rafted microstructure is critical in controlling the creep resistance of single crystal superalloys at 1100°C. At low stresses where dislocations were primarily confined within the γ phase, the Ru addition was particularly effective in extending the creep life of the alloy by suppressing the formation of TCP phase. At slightly higher stresses and correspondingly shorter stress rupture lives, the beneficial effect of Ru was less evident in this particular set of alloys. These results are consistent with the creep response of the alloys at 1000°C, Figure 2, where TCP precipitation was suppressed and the microstructures were identical. Volume fractions of γ' and γ at various creep conditions are summarized in Table II, which shows that at high temperatures (>1000°C), both alloys behave similarly in creep when ratios of overall γ'/γ volume fractions are similar. However, the continuous precipitation of TCP phases in RR2100 at 1100°C 100MPa resulted in localized microstructural changes. As the TCP phases and surrounding envelope of γ' coarsen, the γ' volume fraction begins to decrease in the rafted regions adjacent to the phase instabilities.

This gradual change causes an inversion in the rafted microstructure where isolated rafts of γ' are contained within a matrix of γ , Figure 4a. Where limited microstructural changes occur during the test, the creep responses of the two alloys are essentially identical, as the results in creep condition - 1100°C 175MPa show, Figure 1 and 5.

Both RR2100 and RR2101 have negative lattice misfits between the γ' and γ phases. The addition of Ru increases the lattice parameter of γ more than γ' , which is in agreement with Ru partitioning to the γ phase, Figure 9. The γ' lattice parameter of RR2101 is similar to RR2100 at room temperature, and it increases more rapidly with the addition of Ru as the temperature increases. This is consistent with the finding in a previous study [11], which had established the effects of Ru in lowering the γ' solvus. As the temperature increases, the γ phase expands faster than the intermetallic γ' , causing the lattice misfit to become more negative. Between room temperature and 1100°C, the lattice misfit for RR2100 and RR2101 increased to -0.242% and -0.281%, respectively, Figure 8(b).

The systematic change of measured misfit values with temperature for both alloys appears to be less than that of CMSX-4 [14]. The larger misfit in RR2101 does not seem to contribute

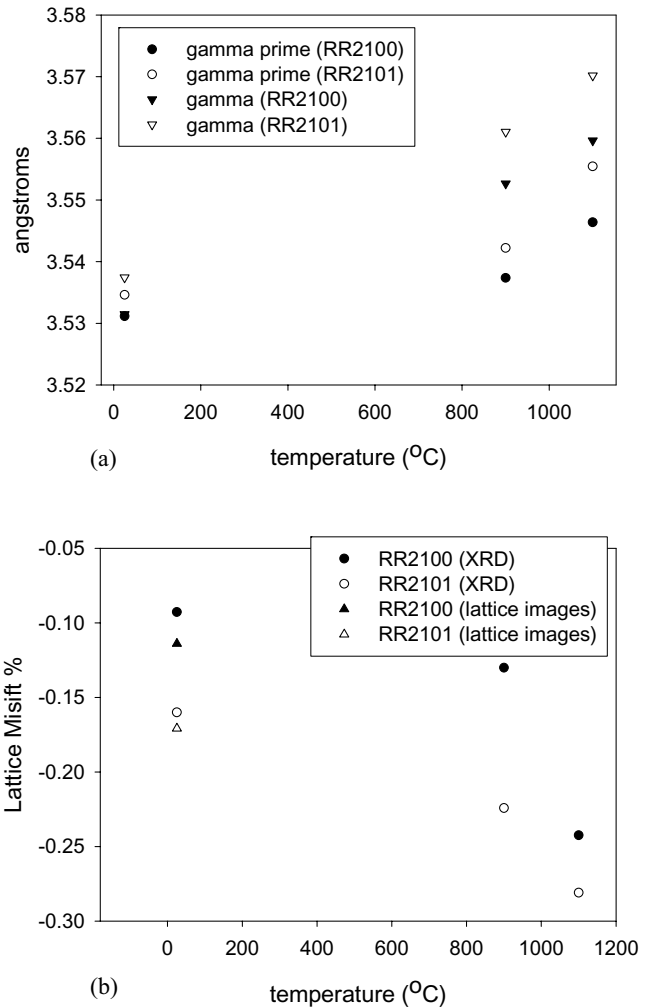


Figure 8. (a) Lattice parameters estimated from XRD scans and (b) Lattice misfit values calculated at room temperature, 900°C and 1100°C for both RR2100 and RR2101

significantly to the overall improvement in creep response when compared to RR2100 under these conditions. For the specific temperature and loading conditions investigated, the corresponding minimum creep strain rates for RR2101 are all

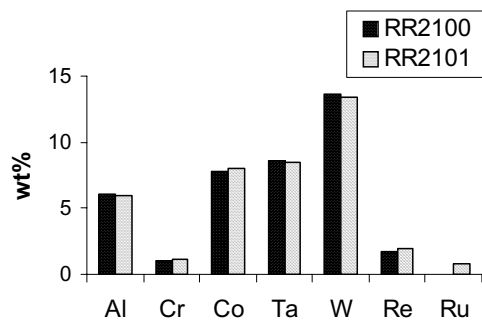


Figure 9. Gamma prime compositions were determined by TEM-EDX, results shown are consistent with wet chemical analysis and atom probe microanalysis [13].

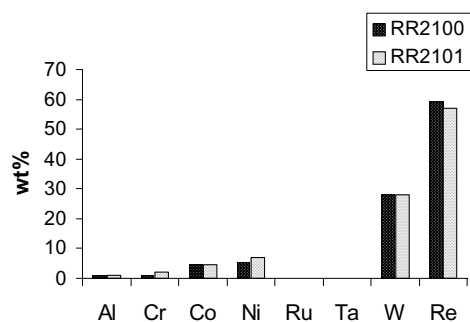


Figure 10. TEM-EDX analysis showed that P phase in both alloys have very similar composition, and Ru was not detected in the P phase of RR2101.

lower than values of RR2100, Figure 3. This observation is consistent with analysis of results from lattice misfit measurements. Studies [12] have suggested that higher lattice misfit results in a denser dislocation network that can provide a certain degree of strengthening as well as hinder the coarsening of the γ' precipitates. Ru-containing RR2101 exhibits a finer dislocation network, however, the difference in dislocation spacing does not seem to have strong influence on overall creep rupture life in present study. Investigations are currently underway to determine the underlying mechanisms as to how Ru restricts the formation of TCP phases. The present investigation reveals that Ru additions do not significantly change the γ'/γ composition, Figure 9. Changes in the partitioning behavior of the alloying elements between the γ and γ' phases [15] were not evident in these experimental alloys. Moreover, Ru itself is not a TCP forming element, Figure 10.

In accordance with the time-temperature-transformations of TCP phases [11], the present study highlights the indirect benefit of Ru additions in hindering the precipitation of TCP phases. This is the primary factor leading to the much improved creep resistance at 1100°C and 100MPa. Changes in lattice misfit and characteristic of the dislocation networks due to Ru were also observed at all creep conditions investigated, however, the effect on the overall creep life appears to be minimal. Although Ru partitions to γ , Ru does not seem to be an effective solid solution strengthener, as the

creep response of the two alloys is similar when microstructures are identical. In addition to influencing the solidification characteristics and phase stability of high refractory content Ni-base superalloys, the presence of Ru also impacts the manner in which the microstructure evolves to accommodate deformation at elevated temperatures. Although the rafted microstructures formed in both alloys at 1100°C are resistant to deformation at loads below 100 MPa, precipitation of TCP phases in RR2100 leads to a rapid degradation of creep properties. The rafted microstructure in RR2101, which is resistant to TCP formation, remains stable and little deformation occurs even after 900 hours. At higher stresses or at lower temperatures where creep properties are less dependent upon the formation of TCP phases, the effects of Ru are less pronounced.

Conclusion

The high temperature creep behavior (>1000°C) of a Ru-bearing Ni-base single crystal superalloy has been investigated and compared to a nominally identical alloy without Ru. The following conclusions regarding the effect of Ru additions on the high temperature creep properties can be drawn from this study:

(1) Additions of Ru improve microstructural stability at high temperatures by hindering the formation of TCP phases and maintaining the continuity of the rafted microstructure. This phenomenon indirectly improves the creep resistance at high temperatures and low loads.

(2) A higher misfit in the Ru-bearing alloy correlates well with the finer dislocation spacings and lower minimum creep strain rates. However, in the present set of alloys where the high temperature creep properties are strongly dependent upon microstructural stability, the associated changes in lattice misfit are not contributing significantly to the overall creep performance of the alloy.

(3) Similar creep responses of RR2100 and RR2101 at lower temperature or higher loads imply that Ru itself does not appear to provide much strengthening.

References

1. F.R.N. Nabarro and H.L. de Villiers, *The Physics of Creep* (Taylor & Francis Ltd 1995), 241-248.
2. R.C. Reed, N. Matan, D.C. Cox, M.A. Rist and C.M.F. Rae, "Creep of CMSX-4 Superalloy Single Crystals: Effect of Rafting at High Temperature", *Acta Mater*, 47 (12) (1999), 3367-3381.
3. Frank R.N. Nabarro, "Rafting in Superalloys" *Metallurgical and Materials Transaction A*, 27 (3) (1996), 513-530
4. Grosdidier, T., A. Hazotte, and A. Simon. "About Chemical Heterogeneities and Gamma Prime Precipitate in Single Crystal Nickel Base Superalloys." (High Temperature Materials for Power Engineering 1990. Kluwer, Dordrecht, Netherlands)
5. Rae, C.M.F. and RC Reed, "The Precipitation of topologically close-packed phases in rhenium-containing superalloys." *Acta Materialia*, 49 (2001), 4113-4125

6. R. Darolia, DF Lahrman, and RD Field, "Formation of topologically closed packed phases in nickel base single crystal superalloys", *Superalloys 1988*, 255-264.
7. R. G. Barrows and J.B. Newkirk, "A modified system for predicting σ formation." *Metallurgical and Materials Transactions A*, 3 (11) (1972)2889-2893.
8. J. R. Mihalisin, C. G. Bieber, and R.T. Grant, "Sigma-its occurrence, effect and control in nickel-base superalloys." *Transactions of the Metallurgical Society of the AIME*, 242, 2399-2414, December 1968
9. Q. Feng, T.K. Nandy, S. Tin and T.M. Pollock, "Solidification of High Refractory Ruthenium Containing Superalloys", *Acta Mater.*, 51 (2003), 269 – 284.
10. Yutaka Koizumi, Toshiharu Kobayashi, Tadaharu Yokokawa, Hiroshi Harada, "Development of 4th generation Ni base single crystal superalloys". *High Temperature Materials 2001*, 2001, 30
11. A.C. Yeh, S. Tin, "Solidification and Phase Stability of Ru-bearing Ni-based Superalloys", *Parsons 2003, 16-18 September 2003, Trinity College Dublin, Ireland*, 673-P686.
12. J.X. Zhang, T. Murakumo, Y. Koizumi, T.Kobayashi, H. Harada, and S. Masaki, JR, "Interfacial Dislocation Networks Strengthening a Forth Generation Single-Crystal TMS-138 Superalloy", *Metallurgical and Materials Transactions A*, 33 (2002), 3741
13. S. Tin, A. C. Yeh, A. P. Ofori, R. C. Reed, S. S. Babu, M. K. Miller, "Atomic partitioning of ruthenium in nickel based superalloys." Paper to be submitted to Superalloys 2004.
14. T. Yokokawa, M. Osawa, H. Murakami, T. Kobayashi, Y. Koizumi, T. Yamagata and H. Harada, "High Temperature Measurements of γ'/γ Lattice Misfits in Third Generation Ni-Base Superalloy". *Proc. Of Materials for Advanced Power Engineering 1998*, 5, part II, 1121-1128.
15. K.S. O'Hara, W.S. Walston, E.W. Ross and R. Darolia, United States Patent 5,482,789, 9 January 1996.

